Optical conductivity evidence of clean-limit superconductivity in LiFeAs

R. P. S. M. Lobo,[1,*] G. Chanda,[2,3] A. V. Pronin,[2,4,5] J. Wosnitza,[2,3] S. Kasahara,[6] T. Shibauchi,[6,7] and Y. Matsuda[6]

[1]*ESPCI-ParisTech, PSL Research University; CNRS, UMR 8213; Sorbonne Universités, UPMC Univ. Paris 6; LPEM, 10 rue Vauquelin, F-75231 Paris Cedex 5, France*

[2]*Dresden High Magnetic Field Laboratory (HLD-EMFL), Helmholtz-Zentrum Dresden-Rossendorf, D-01314 Dresden, Germany*

[3]*Institut für Festkörperphysik, Technische Universität Dresden, D-01062 Dresden, Germany*

[4]*A. M. Prokhorov Institute of General Physics, Russia Academy of Sciences, 119991 Moscow, Russia*

[5]*1. Physikalisches Institut, Universität Stuttgart, Pfaffenwaldring 57, D-70550 Stuttgart, Germany*

[6]*Department of Physics, Kyoto University, Kyoto 606-8502, Japan*

[7]*Department of Advanced Materials Science, University of Tokyo, Chiba 277-8561, Japan*

(Received 3 February 2015; revised manuscript received 23 April 2015; published 11 May 2015)

We measured the optical conductivity of superconducting LiFeAs. In the superconducting state, the formation of the condensate leads to a spectral-weight loss and yields a penetration depth of 225 nm. No sharp signature of the superconducting gap is observed. This suggests that the system is likely in the clean limit. A Drude-Lorentz parametrization of the data in the normal state reveals a quasiparticle scattering rate supportive of spin fluctuations and proximity to a quantum critical point.

DOI: 10.1103/PhysRevB.91.174509 PACS number(s): 74.20.Rp, 74.70.Xa, 74.25.Gz

I. INTRODUCTION

Unlike iron-based superconductors of other families, superconductivity, rather than magnetic order, emerges in LiFeAs at zero chemical doping [1,2]. The superconducting transition temperature is rather high ($T_c = 18$ K at ambient pressure) and the electronic structure of LiFeAs shows no signatures of good nesting [3]. Angle-resolved photoemission spectroscopy (ARPES) [3,4], scanning tunneling spectroscopy (STM) [5], neutron-scattering [6], penetration-depth [7,8], and thermal-conductivity [9] measurements suggest multiband superconductivity and full in-plane gaps with no indications of nodes and with either absent [6,9,10] or modest [3,4,11] gap anisotropy.

Usually, LiFeAs samples have a very large residual resistivity ratio. This is a general indication of high sample quality [12–14]. As superconductivity appears in the stoichiometric composition, the properties of LiFeAs are not influenced by doping-induced defects and impurities. The availability of LiFeAs in the form of large high-quality single crystals makes it a prime material for optical investigations.

To date, only Min *et al.* [10] reported on the far-infrared conductivity of LiFeAs. They described their data in the framework of multiple superconducting gaps, and found two fully open gaps at $2\Delta_0 = 3.2$ meV and $2\Delta_0 = 6.3$ meV. These data were further analyzed in terms of Eliashberg theory [15]. STM also finds two homogeneous nodeless gaps, but with values twice as large [5].

In this paper, we study the optical properties of superconducting LiFeAs. The overall response of this material is similar to other FeAs-based superconductors. Upon entering the superconducting state, LiFeAs shows a loss of spectral weight related to the formation of the superconducting condensate with a penetration depth of 225 nm. However, contrary to Min *et al.* findings [10], we do not observe a clear gap signature, suggesting that the system is likely in the clean limit. The high residual-resistance ratio of our sample and the presence of quantum oscillations in samples from the same batch [16] further support this clean-limit picture. In the normal state, a Drude-Lorentz decomposition of the optical conductivity leads to a scattering rate that evolves linearly with temperature, a property observed in other optimally doped pnictide superconductors and suggestive of the proximity to a quantum critical point (QCP).

II. METHODS

High-quality single crystals of LiFeAs were grown by a self-flux method using Li ingots and FeAs powder. The starting materials were placed in a BN crucible, and sealed in a quartz tube. The tube was heated to 1100 °C, then slowly cooled down to 600 °C. The typical linear size of the single crystals obtained was 3 to 5 mm in each direction. dc resistivity measurements, showing $T_c = 18$ K, have been reported earlier [12].

Near normal incidence reflectivity from 20 to 6000 cm^{-1} was measured on Bruker IFS113 and IFS66v spectrometers at 5, 10, 15, 20, 25, 50, 100, 200, and 300 K. The absolute reflectivity of the sample was obtained with an *in situ* gold overfilling technique [17]. The reflectivity has an absolute accuracy better than 0.5% and a relative accuracy better than 0.1%. The data were extended to the visible and UV (5000 to 40 000 cm^{-1}) at room temperature with an AvaSpec-2048 × 14 spectrometer.

LiFeAs is highly air sensitive. To preserve the sample, it was kept in a sealed vial in Ar atmosphere and mounted in the cryostat cold finger inside a glove box, also in Ar atmosphere. The sample was cleaved prior to each temperature run.

III. RESULTS

Figure 1 displays the *ab*-plane reflectivity of LiFeAs above and below T_c. The low-frequency reflectivity increases steadily with decreasing temperature. Contrary to an *s*-wave BCS

*lobo@espci.fr

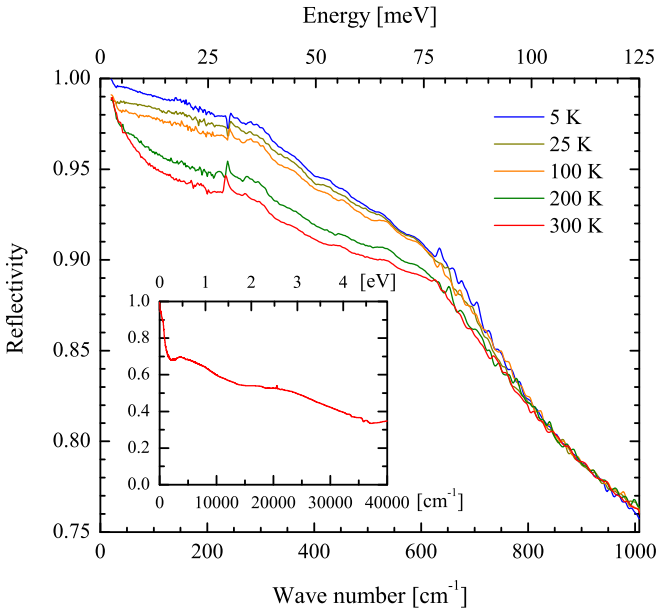

FIG. 1. (Color online) In-plane infrared reflectivity of LiFeAs. The inset shows the reflectivity at 300 K up to 5 eV.

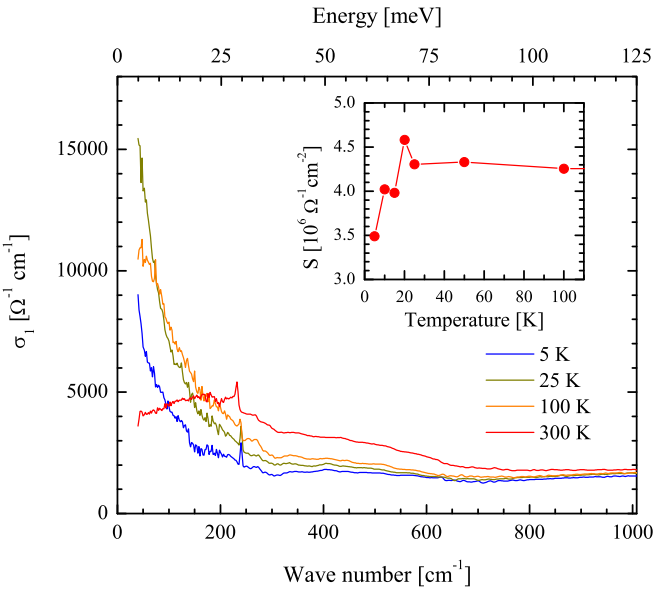

FIG. 2. (Color online) Optical conductivity of LiFeAs above and below T_c. The inset shows the spectral weight below 100 K calculated by integrating σ_1 up to 0.5 eV. Below T_c, it shows a drop related to the formation of the superconducting condensate.

superconductor, there is no sharp rise of the reflectivity upon entering the superconducting state. There is also no sign of a flat 100% reflectivity at low frequencies. The sharp peak around 240 cm^{-1}(30 meV) is a polar phonon of LiFeAs.

The real part, $\sigma_1(\omega)$, of the optical conductivity was derived from the reflectivity through Kramers-Kronig analysis. At low frequencies we utilized either a Hagen-Rubens $(1 - A\sqrt{\omega})$ or a superconducting $(1 - A\omega^4)$ extrapolation. At high frequencies we applied a constant reflectivity to 12.5 eV followed by a ω^{-4} free-electron termination.

Figure 2 shows $\sigma_1(\omega)$ at various temperatures for wave numbers above 40 cm^{-1}, our limit of confidence in Kramers-Kronig obtained data. At 300 K, the optical conductivity signals an almost incoherent transport: it depicts a very broad Drude-like peak as well as a bump around 200 cm^{-1}(25 meV), which could be related to low-energy interband transitions, in particular in view of the presence of shallow bands in LiFeAs [3]. However, we cannot exclude a small surface contamination due to the fragile chemical stability of LiFeAs. We will not discuss this feature any further. When cooling down the sample, in the normal state, the Drude-like term increases and fully develops into a coherent peak. Upon crossing into the superconducting state, the low frequency optical conductivity decreases for energies below 600 cm^{-1}(75 meV). The inset of Fig. 2 shows a sum-rule analysis that is discussed in Sec. V.

IV. CLEAN-LIMIT SUPERCONDUCTIVITY

Looking at Fig. 2, one cannot pinpoint a clearcut sharp energy edge characteristic of an *s*-wave, BCS superconducting gap. There are two main possibilities for the absence of a superconducting gap edge. The first option is a strong anisotropy in the gap, preferably with nodes. Although some anisotropy has been observed by ARPES [3,4] and momentum-resolved tunneling spectroscopy [11], it is too small to account for a nonvanishing low-energy optical conductivity originating from unpaired quasiparticles. Indeed, virtually every measurement of the gap in LiFeAs indicates a nodeless state [3–11].

The second possibility is a superconductor in a clean limit, which seems to be the case for LiFeAs [6,7,9,12]. As pointed out by Kamarás *et al.* [18], one does not see the gap in the optical conductivity of a clean superconductor. To understand this statement, let us remark that, optically speaking, the clean limit corresponds to the case where the quasiparticle scattering rate (τ^{-1}) is small compared to the superconducting gap, i.e., $\tau^{-1} < 2\Delta$. In the Drude model, most of the spectral weight is comprised below τ^{-1}. At the superconducting transition, spectral weight below 2Δ is transferred to a $\delta(\omega)$ function representing the condensate. If 2Δ is larger than τ^{-1} the spectral weight around $\omega = 2\Delta$ is vanishingly small—both in the normal and superconducting states—and thus no clear signature of the gap in the optical conductivity exists. Utilizing the Drude-Lorentz model discussed further in this paper and constraining our fits to respect the temperature dependence of the resistivity, we estimate the low-temperature scattering rate to be close to 3 meV (25 cm^{-1}). Several estimates for the gap value in LiFeAs are available. The smallest value reported is 3 meV ($2\Delta = 25$ cm^{-1}) [10]. Every other estimate and measurement fall into the range between 4 meV (32 cm^{-1}) and 10 meV (80 cm^{-1}) [3–6]. This strongly supports the picture where the absence of a gap signature in the optical conductivity of LiFeAs is a clean-limit effect.

Another confirmation of the clean-limit superconductivity in LiFeAs comes from the analysis of the frequency-dependent penetration depth, $\lambda(\omega) = [\mu_0\omega\sigma_2(\omega)]^{-1/2}$, where μ_0 is the vacuum permeability. For a BCS superconductor of arbitrary scattering, the measured penetration depth (as defined above)

is related to the London penetration depth ($\lambda_L = c/\omega_p$, where ω_p is the free-carrier plasma frequency) in a complex way, with the mean free path being involved in the relation [19]. In terms of optical response, one can show that at frequencies above the scattering rate (but still well below ω_p), $\lambda(\omega)$ coincides with λ_L. This is because the penetration depth at a fixed frequency is defined by the integral response of the carriers at all frequencies below this one. At high enough frequencies (above the scattering rate) the unpaired electrons screen the external field as efficiently as the superconducting currents. Note that, at frequencies above the scattering rate, the unpaired electrons do not scatter. In the clean limit at $T = 0$, there are no unpaired electrons at all; thus the high-frequency value of the penetration depth (the London penetration depth) will span down to zero frequency. Conversely, in the dirty limit, there are some unpaired electrons even at $T = 0$. The response of these electrons appear in $\sigma_1(\omega)$ at frequencies between the gap value and the scattering rate. In this frequency range, the measured penetration depth will deviate from λ_L. The λ_L value will not be recovered at $\omega = 0$ because a part of electrons remains unpaired and does not participate in the field screening [but instead contributes to $\sigma_1(\omega)$].

Figure 3 shows that, at our lowest temperature, the spectrum of $\lambda(\omega)$ is basically flat below 600 cm^{-1}. According to the above, this indicates that our sample is in the clean limit. For comparison, we utilized the parametrization of Zimmermann *et al.* [20] to calculate the frequency dependence for a BCS superconductor with different combinations of optical gap and scattering rate values. Regardless of the gap value, our data correspond to clean-limit calculations.

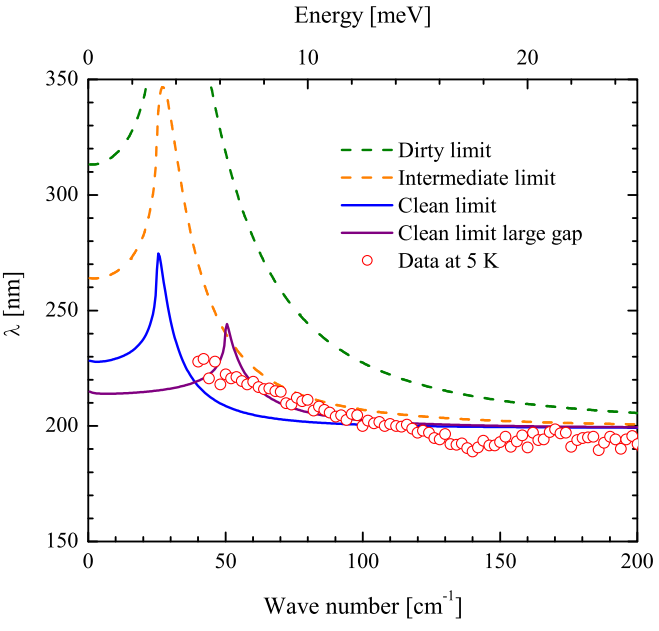

FIG. 3. (Color online) Penetration depth of LiFeAs at 5 K (symbols). The circles are the data and the lines show BCS calculations for the penetration depth. The "Dirty limit" simulation has $2\Delta = 25$ cm^{-1} and $\tau^{-1} = 50$ cm^{-1}. "Intermediate" and "Clean limit" calculations utilize the same value for the gap and τ^{-1} of 25 cm^{-1} and 10 cm^{-1}, respectively. An optical gap of 50 cm^{-1} together with a 10 cm^{-1} scattering rate produce the "Clean limit large gap" simulation.

V. SUM-RULE PENETRATION DEPTH

Rather than the superconducting gap, the important optical signature of the superconducting transition is the loss of spectral weight below T_c, related to the formation of the superfluid condensate. The inset of Fig. 2 shows the spectral weight (S) corresponding to an integration of the optical conductivity up to 4000 cm^{-1} (0.5 eV), below 100 K. In the normal state, this value is constant up to 300 K, within 4%. Below T_c, the occurrence of the superfluid condensate implies a transfer of spectral weight from finite frequencies to a $\delta(\omega)$ function representative of the infinite dc conductivity. As the measured real part of the optical conductivity has no access to zero frequency, the value of its integral drops when the superfluid forms. The difference between the spectral weights in the normal and superconducting states leads to the penetration depth through $\lambda^2 = \pi\varepsilon_0 c^2/[2(S_n - S_{sc})]$, where ε_0 is the vacuum permittivity and the subscripts in S refer to the normal and superconducting states. For LiFeAs, we find $\lambda = 225$ nm at 5 K. This is in very close agreement to values obtained from neutron-scattering (210 nm) [6], infrared (240 nm) [10], transport (210 nm) [12], and muon spin rotation (195 nm) [21] data, as well as with our calculations from $\sigma_2(\omega)$, discussed above and shown in Fig. 3.

VI. NORMAL STATE SCATTERING

Above T_c, $\sigma_1(\omega)$ shows a metallic response which can be modeled by a Drude-Lorentz optical conductivity:

$$\sigma_1(\omega) = \varepsilon_0\left[\frac{\Omega_p^2}{\tau(\omega^2+\tau^{-2})} + \sum_k \frac{\gamma_k\omega^2 S_k^2}{\left(\Omega_k^2-\omega^2\right)^2+\gamma_k^2\omega^2}\right]. \quad (1)$$

The first term in Eq. (1) corresponds to a free-carrier Drude response, characterized by a plasma frequency (Ω_p) and a scattering rate (τ^{-1}). The second term is a sum of Lorentz oscillators characterized by a resonance frequency (Ω_k), a linewidth (γ_k), and a plasma frequency (S_k). Figure 4 shows the result of a fit with Eq. (1) to our data at 100 K. We utilized a Drude peak (hatched red area) to describe the free carriers and four Lorentz terms to account for transitions in the infrared. These five contributions account for the optical conductivity at all temperatures above T_c up to 6000 cm^{-1} (0.75 eV). The scattering rate of the Drude term is the only parameter with a significant temperature dependence. Our Drude fitting parameters were constrained in order to have a temperature dependence of $\sigma_1(0)$ following the inverse dc resistivity.

Although band-structure calculations predict multiple bands at the Fermi level [22,23], one has to consider that the optical conductivity is a reciprocal-space averaged quantity. Therefore, all bands with similar carrier lifetimes will contribute to the same Drude term in σ_1. In this perspective, Wu *et al.* [24] showed that two Drude terms (a narrow one with a small scattering rate and a broad one with a large scattering rate) are sufficient to describe the optical conductivity of most iron-arsenide superconductors. There are two important points

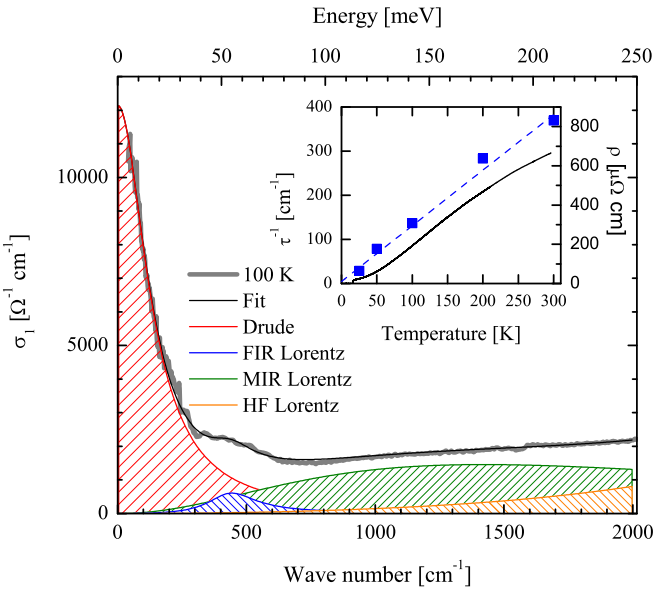

FIG. 4. (Color online) Drude-Lorentz modeling of the optical conductivity of LiFeAs at 100 K. The thick gray line is the data and the thin black line is a fit with a single Drude term ($\Omega_p = 9980$ cm^{-1} and $\tau^{-1} = 137$ cm^{-1}) and four Lorentz terms [far-infrared (FIR), midinfrared (MIR), and two for higher frequencies (HF)]. Individual contributions are shown as hatched areas. The inset shows the temperature dependence of the dc resistivity (solid line), the Drude term scattering rate (squares), and a linear fit to the $\tau^{-1}(T)$ data (dashed line).

to make in this double Drude fitting: (i) most, if not all, of the temperature dependence of the spectra is related to the narrow Drude peak, in particular to its scattering rate, and (ii) the large scattering rate Drude term systematically leads to a mean free path comparable to the lattice parameter. Therefore, the broad Drude term is representative of an incoherent conductivity, probably with bound carriers. In this case, it can be substituted by a Lorentz oscillator with the proper spectral weight. We chose a low-energy Lorentz approach for our fit. This choice is substantiated by the fact that, had we utilized a broad Drude term in our fits, its scattering rate would be around 2500 cm^{-1} (0.3 eV). Taking a Fermi velocity of $\sim$0.4 eV Å [25], one would find a mean free path in the range of 1 Å, which is obviously smaller than the unit cell size. Looking at mobility values reported for LiFeAs [12], one can safely assume that the narrow, coherent, Drude peak is representative of the electron bands.

A multiband analysis of transport data by Rullier-Albenque *et al.* [14] proposes a quadratic temperature dependence for the electron and hole scattering rates in LiFeAs. Their T^2 coefficients are very large, suggestive of strong spin fluctuations. The inset of Fig. 4 shows the temperature dependence of the Drude scattering rate, obtained by fitting the data in the normal state with Eq. (1). We do not have enough temperatures to make a strong claim, but our data seem to be better described by a linear temperature dependence (dashed line), a trend that is also compatible with spin fluctuations. Interestingly, the actual resistivity of LiFeAs (solid line) shows neither a linear, nor a quadratic temperature evolution of τ^{-1}. This fact is related to the multiband character of pnictides. Electronlike and holelike transport properties vary differently with temperature. At low temperatures electron carriers have a dominating role, whereas a crossover regime appears at higher temperatures where electrons and holes have similar mobilities. This seems to be a common trend in optimally doped FeAs-based superconductors [26].

The multiband character of the transport properties, both dc and optical, suggests a material with strong spin fluctuations associated with a competition between magnetism and superconductivity and a possible existence of a quantum critical point. The ground state of (nominally) undoped LiFeAs is a superconductor with no long-range magnetic order. This suggests that spin fluctuations are not important in this material. Indeed, Borisenko *et al.* [3] interpreted their ARPES data in the framework of no static or fluctuating magnetic order. This observation would be at odds with the spin-fluctuations driven superconductivity leading to an $s_{\pm}$ order parameter proposed for iron pnictides in general [27,28], and for LiFeAs in particular [4]. However, a different picture emerges from NMR experiments. Ma *et al.* [29] showed that small deviations from stoichiometry can tune LiFeAs from a material with spin fluctuations to a system with a spin-density-wave QCP. They assign these deviations to the easiness of reversibly intercalating lithium in interstitial sites. This QCP gets further support from the linear temperature dependence of the scattering rate shown in Fig. 4.

VII. SUMMARY

In summary, our optical results show a consistent picture of clean-limit superconductivity in LiFeAs. In the normal state LiFeAs shows an optical conductivity dominated by a narrow Drude-like peak with a strong temperature dependence. When crossing into the superconducting state, this Drude-like peak shows a gradual decrease in its spectral weight, characteristic of a superfluid condensate. From the lost spectral weight, we calculate a penetration depth of 225 nm at 5 K. We did not observe any sharp edge in the spectra, indicating that no superconducting gap signature is observed in the infrared. We conclude that this is a consequence of the system being in the clean limit, a property further confirmed by our detailed analysis of the frequency dependent penetration depth. The normal-state optical conductivity can be parametrized by a Drude-Lorentz dielectric function. We find that all parameters in the Drude-Lorentz model are temperature independent, except for the scattering rate of a coherent Drude peak, representative of quasiparticles on the electron Fermi sheets. A multiband analysis of the scattering rate indicates a non-Fermi-liquid behavior. The linear behavior observed for the scattering rate is compatible with spin fluctuations and supports the presence of a quantum critical point.

ACKNOWLEDGMENTS

Part of this work was supported by HLD at HZDR, member of the European Magnetic Field Laboratory (EMFL).

[1] X. C. Wang, Q. Q. Liu, Y. X. Lv, W. B. Gao, L. X. Yang, R. C. Yu, F. Y. Li, and C. Q. Jin, The superconductivity at 18 K in LiFeAs system, Solid State Commun. **148**, 538 (2008).

[2] J. H. Tapp, Z. Tang, B. Lv, K. Sasmal, B. Lorenz, P. C. W. Chu, and A. M. Guloy, An intrinsic FeAs-based superconductor with $T_c = 18$ K, Phys. Rev. B **78**, 060505(R) (2008).

[3] S. V. Borisenko, V. B. Zabolotnyy, D. V. Evtushinsky, T. K. Kim, I. V. Morozov, A. N. Yaresko, A. A. Kordyuk, G. Behr, A. Vasiliev, R. Follath *et al.*, Superconductivity without nesting in LiFeAs, Phys. Rev. Lett. **105**, 067002 (2010).

[4] K. Umezawa, Y. Li, H. Miao, K. Nakayama, Z.-H. Liu, P. Richard, T. Sato, J. B. He, D.-M. Wang, G. F. Chen *et al.*, Unconventional Anisotropic s-wave superconducting gaps of the LiFeAs iron-pnictide superconductor, Phys. Rev. Lett. **108**, 037002 (2012).

[5] S. Chi, S. Grothe, R. Liang, P. Dosanjh, W. N. Hardy, S. A. Burke, D. A. Bonn, and Y. Pennec, Scanning Tunneling Spectroscopy of Superconducting LiFeAs Single Crystals: Evidence for Two Nodeless Energy Gaps and Coupling to a Bosonic Mode, Phys. Rev. Lett. **109**, 087002 (2012).

[6] D. S. Inosov, J. S. White, D. V. Evtushinsky, I. V. Morozov, A. Cameron, U. Stockert, V. B. Zabolotnyy, T. K. Kim, A. A. Kordyuk, S. V. Borisenko *et al.*, Weak Superconducting Pairing and a Single Isotropic Energy Gap in Stoichiometric LiFeAs, Phys. Rev. Lett. **104**, 187001 (2010).

[7] H. Kim, M. A. Tanatar, Y. J. Song, Y. S. Kwon, and R. Prozorov, Nodeless two-gap superconducting state in single crystals of the stoichiometric iron pnictide LiFeAs, Phys. Rev. B **83**, 100502(R) (2011).

[8] K. Hashimoto, S. Kasahara, R. Katsumata, Y. Mizukami, M. Yamashita, H. Ikeda, T. Terashima, A. Carrington, Y. Matsuda, and T. Shibauchi, Nodal versus nodeless behaviors of the order parameters of LiFeP and LiFeAs superconductors from magnetic penetration-depth measurements, Phys. Rev. Lett. **108**, 047003 (2012).

[9] M. A. Tanatar, J.-P. Reid, S. R. de Cotret, N. Doiron-Leyraud, F. Laliberté, E. Hassinger, J. Chang, H. Kim, K. Cho, Y. J. Song *et al.*, Isotropic three-dimensional gap in the iron arsenide superconductor LiFeAs from directional heat transport measurements, Phys. Rev. B **84**, 054507 (2011).

[10] B. H. Min, J. B. Hong, J. H. Yun, T. Iizuka, S. Kimura, Y. Bang, and Y. S. Kwon, Optical properties of the iron-based superconductor LiFeAs single crystal, New J. Phys. **15**, 073029 (2013).

[11] M. P. Allan, A. W. Rost, A. P. Mackenzie, Y. Xie, J. C. Davis, K. Kihou, C. H. Lee, A. Iyo, H. Eisaki, and T.-M. Chuang, Anisotropic Energy Gaps of Iron-Based Superconductivity from Intraband Quasiparticle Interference in LiFeAs, Science **336**, 563 (2012).

[12] S. Kasahara, K. Hashimoto, H. Ikeda, T. Terashima, Y. Matsuda, and T. Shibauchi, Contrasts in electron correlations and inelastic scattering between LiFeP and LiFeAs revealed by charge transport, Phys. Rev. B **85**, 060503 (2012).

[13] O. Heyer, T. Lorenz, V. B. Zabolotnyy, D. V. Evtushinsky, S. V. Borisenko, I. Morozov, L. Harnagea, S. Wurmehl, C. Hess, and B. Büchner, Resistivity and Hall effect of LiFeAs: Evidence for electron-electron scattering, Phys. Rev. B **84**, 064512 (2011).

[14] F. Rullier-Albenque, D. Colson, A. Forget, and H. Alloul, Multiorbital effects on the transport and the superconducting fluctuations in LiFeAs, Phys. Rev. Lett. **109**, 187005 (2012).

[15] J. Hwang, J. P. Carbotte, B. H. Min, Y. S. Kwon, and T. Timusk, Electron-boson spectral density of LiFeAs obtained from optical data, J. Phys.: Condens. Matter **27**, 055071 (2015).

[16] C. Putzke, A. I. Coldea, I. Guillamón, D. Vignolles, A. McCollam, D. LeBoeuf, M. D. Watson, I. I. Mazin, S. Kasahara, T. Terashima *et al.*, de Haas-van Alphen study of the Fermi surfaces of superconducting LiFeP and LiFeAs, Phys. Rev. Lett. **108**, 047002 (2012).

[17] C. C. Homes, M. Reedyk, D. A. Cradles, and T. Timusk, Technique for measuring the reflectance of irregular, submillimeter-sized samples, Appl. Opt. **32**, 2976 (1993).

[18] K. Kamarás, S. L. Herr, C. D. Porter, N. Tache, D. B. Tanner, S. Etemad, T. Venkatesan, E. Chase, A. Inam, X. D. Wu *et al.*, In a clean high-T_c superconductor you do not see the gap, Phys. Rev. Lett. **64**, 84 (1990).

[19] P. B. Miller, Penetration depth in impure superconductors, Phys. Rev. **113**, 1209 (1959).

[20] W. Zimmermann, E. H. Brandt, M. Bauer, E. Seider, and L. Genzel, Optical conductivity of BCS superconductors with arbitrary purity, Physica C **183**, 99 (1991).

[21] F. L. Pratt, P. J. Baker, S. J. Blundell, T. Lancaster, H. J. Lewtas, P. Adamson, M. J. Pitcher, D. R. Parker, and S. J. Clarke, Enhanced superfluid stiffness, lowered superconducting transition temperature, and field-induced magnetic state of the pnictide superconductor LiFeAs, Phys. Rev. B **79**, 052508 (2009).

[22] I. A. Nekrasov, Z. V. Pchelkina, and M. V. Sadovskii, Electronic structure of new LiFeAs high-T_c superconductor, JETP Lett. **88**, 543 (2008).

[23] D. J. Singh, Electronic structure and doping in $BaFe_2As_2$ and LiFeAs: Density functional calculations, Phys. Rev. B **78**, 094511 (2008).

[24] D. Wu, N. Barišić, P. Kallina, A. Faridian, B. Gorshunov, N. Drichko, L. J. Li, X. Lin, G. H. Cao, Z. A. Xu *et al.*, Optical investigations of the normal and superconducting states reveal two electronic subsystems in iron pnictides, Phys. Rev. B **81**, 100512 (2010).

[25] H. Ding, K. Nakayama, P. Richard, S. Souma, T. Sato, T. Takahashi, M. Neupane, Y. M. Xu, Z. H. Pan, A. V. Fedorov *et al.*, Electronic structure of optimally doped pnictide $Ba_{0.6}K_{0.4}Fe_2As_2$: A comprehensive angle-resolved photoemission spectroscopy investigation, J. Phys.: Condens. Matter **23**, 135701 (2011).

[26] Y. M. Dai, B. Xu, B. Shen, H. Xiao, H. H. Wen, X. G. Qiu, C. C. Homes, and R. P. S. M. Lobo, Hidden T-linear scattering rate in $Ba_{0.6}K_{0.4}Fe_2As_2$ revealed by optical spectroscopy, Phys. Rev. Lett. **111**, 117001 (2013).

[27] I. I. Mazin, D. J. Singh, M. D. Johannes, and M. H. Du, Unconventional superconductivity with a sign reversal in the order parameter of $LaFeAsO_{1-x}F_x$, Phys. Rev. Lett. **101**, 057003 (2008).

[28] V. Cvetkovic and Z. Tesanovic, Multiband magnetism and superconductivity in Fe-based compounds, EPL **85**, 37002 (2009).

[29] L. Ma, J. Zhang, G. F. Chen, and W. Yu, NMR evidence of strongly correlated superconductivity in LiFeAs: Tuning toward a spin-density-wave ordering, Phys. Rev. B **82**, 180501 (2010).